Hue shifts produced by temporal asymmetries in chromatic signals

Andrew Stockman UCL Institute of Ophthalmology, University College London, London, UK

G. Bruce Henning UCL Institute of Ophthalmology, University College London, London, UK

Peter West UCL Institute of Ophthalmology, University College London, London, UK

Andrew T. Rider UCL Institute of Ophthalmology, University College London, London, UK

Hannah E. Smithson Department of Experimental Psychology, University of Oxford, Oxford, UK

Caterina Ripamonti UCL Institute of Ophthalmology, University College London, London, UK

Observers viewed M- or L-cone-isolating stimuli and compared slowly-on and slowly-off sawtooth waveforms of the same mean chromaticity and luminance. Between 6 and 13 Hz, the mean hue of slowly-on L-cone and slowly-off M-cone sawtooth flicker appeared redder, and the mean hue of slowly-off L-cone and slowly-on M-cone sawtooth stimuli appeared greener—despite all the waveforms' having the same mean, near-yellow-appearing chromaticity. We measured the effect of the modulation depth and the slope of the sawtooth on the mean hue shifts as a function of temporal frequency. The results are complex but show that discriminability depended mainly on the second harmonic of the waveforms. We considered several models with combinations of linear and nonlinear stages. First, we considered models in which a nonlinear stage limits the rate of change of hue and restricts the steep slope of the sawtooth waveform more than its shallow slope, thus shifting the mean hue in the direction of the shallower slope (such a nonlinearity is also known as a *slew-rate* limit). Second, we considered *saturation* models in which the nonlinear stage compresses hue signals and thus shifts the mean of asymmetrical waveforms with or without differentiation before the nonlinearity. Overall, our modeling and results suggest that the hue shift occurs at some nonlinear mechanism in the chromatic pathway; and that, in terms of the Fourier components of the various waveforms, the effect of the nonlinearity depends crucially on the timing of the second harmonic relative to the first.

Introduction

The functions relating modulation or contrast sensitivity to temporal frequency are known as temporal contrast-sensitivity functions (TCSFs). The frequency-dependence of sensitivity to temporally modulated *chromatic* flicker is characteristically *low-pass* in shape; sensitivity is roughly constant at low and intermediate frequencies but, at high frequencies, falls steeply with increasing frequency. In contrast, the sensitivity to *luminance* or *achromatic* flicker is characteristically *band-pass*; sensitivity peaks at some intermediate frequency and falls at frequencies both above and below the peak. The high-frequency falloff of luminance or achromatic flicker is much shallower than that of chromatic flicker. One consequence of these frequency-dependent differences is that observers are typically more sensitive to chromatic flicker at low frequencies and more sensitive to achromatic flicker at high frequencies. There is an extensive literature on the temporal characteristics of chromatic and achromatic flicker (e.g., de Lange, 1958; Walraven & Leebeek,

Citation: Stockman, A., Henning, G. B., West, P., Rider, A. T., Smithson, H. E., & Ripamonti, C. (2017). Hue shifts produced by temporal asymmetries in chromatic signals. *Journal of Vision*, *17*(9):2, 1–21, doi:10.1167/17.9.2.

doi: 10.1167/17.9.2 Received March 23, 2017; published August 2, 2017 ISSN 1534-7362

1964; Brindley, Du Croz, & Rushton, 1966; Green, 1969; Regan & Tyler, 1971; King-Smith, 1975; King-Smith & Carden, 1976; Kelly & van Norren, 1977; Tolhurst, 1977; Sternheim, Stromeyer, & Khoo, 1979; Noorlander, Heuts, & Koenderink, 1981; Smith, Bowen, & Pokorny, 1984; Stockman, MacLeod, & DePriest, 1991; Metha & Mullen, 1996).

Standard linear systems approaches to modeling the visual system often consider visual processing in terms of cascades of linear filters with or without feedback or feed-forward. In these models, TCSFs are treated as reflecting the attenuation characteristic of the cascade (for review, see Watson, 1986). Thus, the additional losses of sensitivity at high temporal frequencies in the chromatic system are usually attributed either to extra filtering stages or to stages with longer time constants, both of which increase temporal integration times (e.g., Yeh, Lee, & Kremers, 1995; Lee, Sun, & Zucchini, 2007). Crucially for the observations that follow, the mean (time-averaged) response of a cascade of linear filters, which has reached its steady-state response to a periodic stimulus, depends only on the mean (or time-average) of the stimulus, and not on the stimulus waveform. Thus, the mean color appearance should not depend on the slopes of stimulus waveforms with the same means. For a change in the mean appearance to occur, either a nonlinearity must be introduced into the system, or the stimulus, since its effective duration must be limited, must produce a visible and long-lasting transient at its onset or offset.

Here, we describe and investigate a color phenomenon that is inconsistent with simple linear-systems' models. Observers viewed lights that flickered in a sawtooth temporal pattern. The flickering lights had waveforms that were either *slowly-on*/*rapidly-off* or *slowly-off*/*rapidly-on*. We used stimuli that were designed to excite either only the long-wavelength–sensitive (L-) cones or only the middle-wavelength–sensitive (M-) cones. Similar M- and L-cone contrasts were used. The observers reported that between about 6 and 13 Hz, there were shifts in the mean hue of sawtooth waveforms in the direction of the *slowly* changing ramp of the sawtooth. Thus, the mean hue of sawtooth flicker modulated along a red–green axis shifts toward red if the slow ramp is from green to red, whereas it shifts toward green if the slow ramp of the sawtooth is from red to green. These shifts are seen despite the two waveforms having the same mean chromaticity, the same mean luminance, and, indeed, the same amplitude spectrum since the slowly-off waveform is just the slowly-on waveform played backward. Because L- and M-cone modulations were used, there were also luminance variations, but the dominant perceptions were changes in hue rather than changes in brightness or saturation. The mean response of a linear system depends only on the mean of the input signal and the gain of the system at 0 Hz, and not on the time-varying components of the signal. Thus, a linear systems model does not easily predict the changes in mean hue appearance that we find with time-varying signals of equal mean.

Our initial approach to understanding this phenomenon was to measure the dependence of the mean hue change on the depth of the sawtooth modulation and then on the steepness of the rising and falling slopes both as a function of frequency; and then to model those dependencies. Our results suggest that the first and second harmonics of the waveforms are the most significant in understanding the effect.

General methods

This research adhered to the tenets of the Declaration of Helsinki. Various types of psychophysical methods were employed, including spatial and temporal two-alternative forced choice and method-of-adjustment, as well as phenomenological reports.

Observers

Four female (CN, KR, ME, and MS) and three male observers (JA, VL, and AS) participated. All were experienced psychophysical observers with normal color vision and normal spatial acuity as determined by standard tests. Two of them, KR and AS, were authors (KR is Caterina "Katia" Ripamonti). Three additional naïve observers with normal color vision were asked to make subjective observations on the appearances of the sawtooth waveforms.

Maxwellian-view system

Although most of the stimuli were presented using a cathode ray tube (CRT), our initial observations were obtained using a standard Maxwellian-view optical system. Given the importance of establishing that the color phenomena we explored were not dependent on the method of stimulus generation, we briefly describe the Maxwellian-view system and its use. Full details of the system can be found elsewhere (Stockman, Sharpe et al., 2007; Stockman, Smithson et al., 2007; Stockman et al., 2008).

The Maxwellian-view system had five channels all illuminated by a 900-W Xe arc lamp. The radiance in each channel was controlled by the insertion of fixed neutral density filters (Ealing, Holliston, MA; Oriel, Stratford, CT, or Melles Griot, Irvine, CA) or by the rotation, under computer control, of circular, variable,

neutral-density filters (Rolyn Optics, Covina, CA). Wavelengths were selected by interference filters with full-width-at-half-maximum bandwidths of between 7 and 11 nm (Ealing or Oriel). Sawtooth and other flickering waveforms were produced by pulse-width modulation of fast, ferro-electric liquid crystal light shutters (Displaytech, Longmont, CO) at a carrier frequency of 400 Hz. Frequencies near the 400-Hz rectangular-pulse frequency were much too high to be resolved, so that observers saw only the temporally changing stimuli produced by the variation of the pulse width. The desired sawtooth and triangular waveforms were calculated in real time using counters and loops. The maximum rise-time for the sawtooth flicker was 2.5 ms (i.e., the period of the 400-Hz carrier) and the maximum usable contrast for a given channel was 92%. Head positions were maintained by a dental bite bar and viewing was monocular.

We refer to the magnitude of each stimulus as the *depth of modulation* or the *modulation* for short. By that, we mean the ratio of the maximum deviation of the waveform to its mean, usually expressed as a percentage. For a given cone type, the cone modulation is thus the ratio of the maximum cone excitation produced by the waveform to the mean cone excitation produced by the waveform, again usually expressed as a percentage. This can be calculated simply from the stimulus calibrations using the CIE cone fundamentals of Stockman and Sharpe (2000).

In the Maxwellian-view system all five channels were optically superimposed and used to produce circular targets, the diameter of which subtended 4° of visual angle. The specific wavelengths in each channel were chosen to isolate either L- or M-cones responses, and to have little effect on S-cones. To produce L-cone-isolating waveforms, a 650-nm target of 9.49 $\log_{10}$ quanta s^{-1} deg^{-2} and a 521-nm target of 7.68 $\log_{10}$ quanta s^{-1} deg^{-2} were modulated in opposite phase (the two lights were M-cone equated, so produced little or no M-cone flicker). A 520-nm target of 8.52 $\log_{10}$ quanta s^{-1} deg^{-2} and a 658-nm target of 9.40 $\log_{10}$ quanta s^{-1} deg^{-2} were flickered in opposite phase to produce M-cone–isolating flicker (these two lights were L-cone equated, so produced little or no L-cone flicker). The relative radiances to equate the targets for either L- or M-cone isolation were based on the CIE cone fundamentals of Stockman and Sharpe (2000). The calculated maximum L-cone and M-cone modulation was about 15% in both cases. Because the combined targets appeared orange when unmodulated, a fifth, steady 529-nm target of 8.90 $\log_{10}$ quanta s^{-1} deg^{-2} was added to make the mean hue in the absence of flicker more yellow, although while some observers saw the unmodulated target as yellow, others saw it as slightly orange. The overall retinal illuminance was approximately 3.06 $\log_{10}$ photopic trolands, thus precluding rod involvement (Sharpe, Fach, Nordby, & Stockman, 1989).

Observers preadapted to the unmodulated stimuli in Maxwellian-view or on the CRT for 2 min prior to making observations.

CRT and VSG system

For forced-choice and later method-of-adjustment measurements, we used a calibrated 21 in. Sony FD Trinitron CRT and VSG2/5 Visual Stimulus Generator (Cambridge Research Systems Ltd., Rochester, Kent, UK). The CRT and VSG system provides an intensity resolution of up to 14-bits per gun. Each of the red, green, and blue guns of the monitor was individually linearized using a ColorCAL colorimeter (Cambridge Research Systems Ltd.) to measure the luminance of each phosphor and for daily calibration of the experimental conditions. A Radoma spectroradiometer (Gamma Scientific, La Jolla, CA) was used to measure the spectral power distributions of each of the three CRT primaries.

The refresh rate of the monitor was set to 160 Hz (or to 100 Hz for the 0.63-Hz stimulus) with a spatial resolution of 800 × 600 pixels. The timing of stimulus presentation was implemented by the VSG system and was independent of the operating system on the host PC. A six-key response box was used to collect the observers' responses.

Observers sat one meter from the CRT on which the main stimuli were 5.7° diameter semicircular hemifields, separated by a vertical gap of 0.6° visual angle and viewed binocularly through natural pupils. The mean overall luminance was 42.39 cd/m^2. Simple waveforms, such as the sawtooth and square wave, were calculated in real time; other waveforms, such as sinusoids, were precalculated, sampled at the frame rate, and displayed on the linearized CRT.

The stimulus frequencies were chosen to have an integer number of frames in the waveform period and frequencies from 1 to 20 Hz were produced at the 160-Hz frame rate, the 0.63-Hz stimulus was produced at a frame rate of 100 Hz. (Note that any change in the stimulus requires one frame to occur. Thus, the rapid phase of the sawtooth waveforms from 1 to 20 Hz always took at least 6.25 ms (10 ms for the 0.63-Hz flicker) and this quantization is taken into account when calculating the slopes in the variable slope Experiment II.) In forced-choice experiments, the flickering waveforms were turned on and remained on until the observers had made a judgment about which half field appeared redder. The mean perceived hue of the waveforms tended to change slowly, and to persist until the end of the viewing period.

Name	Formula	Equation
Slowly-on sawtooth	$A(t) = \frac{2}{\pi}\left(\sin(2\pi ft) - \frac{1}{2}\sin(2\pi 2ft) + \frac{1}{3}\sin(2\pi 3ft) - \ldots\right)$	1
Slowly-off sawtooth	$A(t) = \frac{2}{\pi}\left(\sin(2\pi ft) + \frac{1}{2}\sin(2\pi 2ft) + \frac{1}{3}\sin(2\pi 3ft) + \ldots\right)$	2
Triangle	$A(t) = \frac{8}{\pi^2}\left(\sin(2\pi ft) - \frac{1}{9}\sin(2\pi 3ft) + \frac{1}{25}\sin(2\pi 5ft) - \ldots\right)$	3
Sine wave	$A(t) = \sin(2\pi ft)$	4
Square wave	$A(t) = \frac{4}{\pi}\left(\sin(2\pi ft) + \frac{1}{3}\sin(2\pi 3ft) + \frac{1}{5}\sin(2\pi 5ft) + \ldots\right)$	5

Table 1. Low- frequency Fourier components of sawtooth and other waveforms.

Cone modulations were around a yellow point (CIE $x = 0.436$; $y = 0.489$) with a luminance of 42.39 cd/m^2. We used a yellow rather than a white background to exclude S-cone involvement. The pupil size was not controlled but with the 3-mm diameter pupil appropriate for this luminance (e.g., Watson & Yellott, 2012), the target would have had a mean retinal illuminance of 2.18 $\log_{10}$ photopic trolands. The phosphors at their maximum intensities were Red: $x = 0.615$, $y = 0.343$ and 28.33 cd/m^2; Green: $x = 0.283$; $y = 0.611$ and 60.26 cd/m^2; and Blue: $x = 0.154$; $y = 0.079$ and 10.43 cd/m^2.

Standard methods were again used for generating cone-isolating stimuli: The spectral power distribution of the three phosphors were multiplied by the Stockman and Sharpe (2000) cone fundamentals and the phosphor combinations that produced silent substitutions for each cone type (Estévez & Spekreijse, 1982) calculated. M- and L-cone modulations of up to about 25% could be achieved for both cone types with the CRT and VSG system (the L-cone modulation was limiting).

Curve fitting

Curve fitting was used both to analyze the data and to evaluate models. For the psychometric functions relating performance to modulation depth or to slope, maximum-likelihood fits of logistic functions were used purely for convenience of description (Wichmann & Hill, 2001a, 2001b). All other fits minimized the sum of the squared differences between the data and model predictions. The latter procedure used the standard nonlinear Marquardt-Levenberg curve-fitting algorithm implemented in Sigmaplot (Systat, San Jose, CA).

Fourier components of the waveforms

We used the Fourier-series components of the various periodic waveforms to help understand the hue-shift phenomenon. In particular, given the results of Experiment I described next, we wished to consider how the sinusoidal components of the stimuli were selectively filtered within the chromatic visual pathway.

Table 1 gives the equations for the first three harmonics of our standard stimuli as a function of frequency (f, Hz) as well as the spectra for sine and square waves. Note that harmonics above the fifth are unlikely to be perceptually salient for most chromatic stimuli except when very low fundamental frequencies are used and that, in Table 1, all the waveforms have an amplitude of 1 and the same mean value.

With the exception of the sine wave, the waveforms we used contain non-zero harmonics that decrease in amplitude with increasing frequency. The frame rate of the CRT of 160 Hz (used for stimulus frequencies $>$ 0.63 Hz), and the carrier frequency of 400 Hz for pulse-width modulation used in the Maxwellian-view system, place the Nyquist frequencies, above which sinusoids will produce aliasing, at 80 and 200 Hz, respectively. Thus, for mean hue shifts for fundamental frequencies of up to 13.33 Hz, the frequency range of interest, only the seventh harmonic exceeds the Nyquist frequency and then only using the CRT. Control experiments in which the higher harmonics of the waveforms were removed showed that they had no visible effect. In fact, above about 5 Hz in our experiments, only the first and second harmonics of these waveforms seemed visually significant.

Simulations

In a linear time-invariant system, sinusoidal inputs produce sinusoidal outputs of the same frequencies but with, in general, different amplitudes and phases. However, both a slew-rate limit and a saturation distort sinusoidal inputs to produce components at frequencies that were not present at the input, and so are inherently nonlinear processes. Because the slew-rate model and saturation models are nonlinear, we cannot employ standard linear systems techniques to understand and predict their behavior. Therefore, to provide some insight, we have used simulations implemented in Simulink and Matlab (MathWorks, Natick, MA). The simulations can be done straightforwardly by generating the waveforms using Matlab functions (e.g., square, sine, sawtooth) and then passing the waveforms through the Simulink Rate Limiter or Saturation function blocks. The output can then be viewed using

the Scope function block, or variously analyzed using Simulink function blocks or Matlab functions. The input and output signals shown in Figures 7 and 8, below, are copied directly from Matlab. Other function blocks can be used to develop the model.

Formally, a slew-rate limited mechanism applied to a discrete time signal $x[n]$ produces an output $y[n]$ such that:

$$y[0] = x[0]$$
$$y[n] = \begin{cases} y[n-1] + S, \text{ if } x[n] > y[n-1] + S \\ y[n-1] - S, \text{ if } x[n] < y[n-1] - S \\ y[n] = x[n], \text{ otherwise,} \end{cases} \quad (6)$$

where S is the slew rate limit and n indexes the discrete time variable. A slew-rate limit cannot be implemented as a linear filter.

Initial subjective observations

Basic phenomenon

Five observers, two of whom (KR and AS) were experimenters, viewed the L- and M-cone modulated waveforms in Maxwellian view at frequencies from 6 to 14 Hz and were asked to provide a subjective description of what they saw. No attempt was made at an objective rating scale, nor did the experimenters suggest hue terms to the observers. There was surprising consistency in the descriptions across observers, which we summarize next. It should be recognized, however, that these are merely subjective descriptions.

At 4 Hz and below, the L- and M-cone modulated waveforms were reported mainly as hue variations between reddish and greenish with no easily described mean hue appearance. Between 6 and 10 Hz, observers consistently reported that the mean hue of the sawtooth waveforms depended on whether the flicker was slowly-off (rapidly-on) or slowly-on (rapidly-off) even though the two types of flicker have the same mean chromaticity, the same mean luminance, and the same Fourier amplitude spectra (see Table 1). In general, the change in hue was in the direction of the slow change in the sawtooth. Thus, for sawtooth waveforms with L-cone slowly-off, and M-cone slowly-on, the change in hue was towards green (i.e., lower L-cone and greater M-cone excitation), while for sawtooth stimuli with M-cone slowly-off and L-cone slowly-on, the change in hue was toward red (i.e., lower M-cone and greater L-cone excitation). The mean hue appearance of triangular flicker depended on the observer and was yellow or orange or pale orange, consistent with the steady (nonflickering) hue appearance.

At 12 Hz, the change in the mean hue of sawtooth flickering light was clear only for some waveforms and cone types, while at 14 Hz (and above) the sawtooth waveforms appeared similar to triangular waveform with no mean hue shift.

Observations made with the CRT monitor and VSG also using 15% L- and M-cone modulations were broadly consistent with those reported in Maxwellian view despite the luminance of the stimuli being about 7.5 times lower. With the CRT, the change in mean color was most striking between 5 and 13 Hz, with the direction of the change again being in the direction of the slow side of the sawtooth waveform. At frequencies below 5 Hz, as in the Maxwellian-view system, hue variation between red and green at the fundamental frequency dominates the color appearance. At frequencies above about 12 Hz, changes in the mean hue, if any, are very small.

With the CRT, we also observed the effect on the appearance of L- and M-cone sawtooth flicker of systematically varying the cone modulation from low levels up to 25% modulation. At lower cone modulations that produce a hue difference between slowly-off and slowly-on sawtooth stimuli, the observers report mainly a flickering reddish-orange hue (for slowly-on L-cone and slowly-off M-cone waveforms) or a flickering greenish hue (for slowly-on M-cone and slowly-off L-cone waveforms). As the modulation is increased, the predominantly greenish or reddish hues appear more saturated and intense, but become interspersed with brief flashes of the opponent green or red hue. Thus, for slowly-on L-cone and slowly-off M-cone sawtooth waveforms the predominantly reddish-orange hue is interspersed with brief green flashes, while for slowly-on M-cone and slowly-off L-cone sawtooth waveforms the predominantly greenish hue is interspersed with brief orange flashes. The brief flashes appeared irregular in time and blotchy in space, possibly because they were not seen during some waveform cycles. In these cases, the appearance of the two opponent hues seem to be mutually exclusive, so that at any one time a patch of the target appeared either greenish or reddish. Consequently, the target sometimes took on a mottled appearance with irregularly placed adjacent patches briefly taking on opposing hues. This description is reminiscent of one of the three subjective reports of the appearance of juxtaposed red and green fields after a retinally stabilized border between them has faded: "(iii) the field may appear as a series of islands of one color on a background of the other color" (Crane & Piantanida, 1983, p. 1079). Under comparable conditions, Billock, Gleason, and Tsou (2001) reported similarly "spatially-structured phenomena" (p. 2399), but when the red and green fields were explicitly set to be nonequiluminant.

In the Maxwellian-view system, interspersed opponent flashes were seen mainly for those sawtooth waveforms that caused a shift in the mean hue towards

green rather than towards red. This may be accounted for by the range of available cone modulations and if slightly higher cone modulations had been used, we might have seen opponent flashes for sawtooth waveforms that shift the mean hue toward red as well. It might also be related to the higher mean luminances used in the Maxwellian-view system or to the more rapid rise and fall times for the rapid slopes in that system.

Experiment I: The temporal contrast sensitivity of the hue-shift discrimination

Introduction

In this experiment, we measured the temporal contrast sensitivity function (TCSF) for detecting the mean hue-shift and compared it with more conventional measurements of TCSFs measured both with sinusoidal L- and M-cone cone-isolating stimuli, and with chromatic flicker.

Methods

Temporal contrast sensitivity for discriminating changes in mean hue: Variable-modulation experiment

We used a two-alternative spatial forced-choice (2AFC) method to determine the modulation at which the observers could discriminate which of two hemifields contained slowly-on flicker presented in one randomly chosen hemifield. The other hemifield contained slowly-off flicker of the same frequency, the same modulation, the same mean chromaticity, and the same luminance. The pairs of sawtooth waveforms were displayed on the CRT in two 5.7° diameter semicircular hemifields separated by 0.6° of visual angle and remained flickering until the observer responded. (Other hemifield sizes were used, but the hue shift is more readily visible on the large field.) There were two conditions: either the L-cones or the M-cones were modulated in isolation. For L-cone modulation, the hemifield containing the slowly-on flicker looked redder; whereas with M-cone stimuli, the slowly-off stimuli looked redder. Observers were simply asked to indicate which hemifield appeared redder. We chose one of the waveforms to be "correct" but no feedback was given. The modulations of the slowly-on and slowly-off pairs were varied together to generate psychometric functions relating the proportion of "redder" responses to the magnitude of the cone modulation for flicker frequencies ranging from 2 to 20 Hz. On each trial, the slowly-on waveform was randomly assigned to one of the hemifields—50% of the time on the left and 50% on the right.

Onset transients

At stimulus onset in the main experiment, the ramps that defined the sawtooth waveforms were always started at the beginning of the slowly rising or slowly falling ramp of the sawtooth. This was done mainly for programming convenience, but it also meant that any onset transient was in the hue direction *opposite* to the direction of the observed mean hue shift, so that it is unlikely that the hue-shift phenomenon can be simply due to the onset transient. This conclusion was borne out by informal observations, made before the experiments, that the persistent hue shift is independent of stimulus onset phase.

Nonetheless, since onset transients could, in principle, cause a hue shift away from the mean, and preserve a linear systems explanation of this phenomenon, we carried out a more formal control experiment on two observers (VL and AS; the original observers KR and JA were no longer available). Contrast sensitivity for detecting the mean hue shift was measured under three conditions: (a) with the stimulus onset at the *beginning* of the slowly rising or falling ramps of the sawtooth (as in the experiment), (b) with the stimulus onset at the *middle* of the slowly rising or falling ramp, and (c) with the modulation at stimulus onset also at the beginning of the slowly rising or falling ramp of the sawtooth, but with the stimulus gradually increasing from and then decreasing to zero following the form of a raised-cosine window. (The modulation on a given trial was multiplied by this raised-cosine window.) The raised-cosine window was a single period of a cosine function that grew sinusoidally from a trough of 0 to a peak of 1 and then fell back to a trough of 0. The period of the raised-cosine was 2 s, so the time from onset to peak modulation was 1 s. Two-alternative forced choice was used either using the method limits (as in the main experiment) or using a standard staircase that tracked 75% correct.

Temporal contrast sensitivity for cone-isolating and chromatic sinusoidal flicker

In addition to the discrimination measurements described above, we measured L- and M-cone-isolating TCSFs with cosine-windowed sinusoidal flicker, and also chromatic TCSFs again with cosine-windowed sinusoidal chromatic flicker in standard temporal 2AFC experiments, using independent dual staircases. The period of the raised-cosine was again 2 s. The targets were circular fields of 5.7° in diameter and the sinusoidal modulation was around the yellow chromaticity. In these experiments, the sinusoidal modulation appeared randomly in one of two 2-s intervals,

indicated by tones, and separated by a 1-s pause. After a "ballpark" setting of 3 reversals with a step size of 0.5 $\log_{10}$ units, the modulation in each staircase decreased by 0.2 $\log_{10}$ units when the observer correctly identified the interval in which the modulation occurred on two successive trials and increased by the same amount if the observer incorrectly identified the interval in which the modulation occurred on any single trial. This procedure ultimately tracks 70.7% correct (Levitt, 1971). Feedback was given in these experiments. Thresholds were taken as the average of the final five modulations visited on each staircase.

Temporal contrast sensitivity was measured using: (a) M-cone-isolating flicker, (b) L-cone-isolating flicker, and (c) chromatic flicker. Chromatic flicker was produced by flickering equiluminant red and green appearing sinusoids in opposite phase. The principle of using equiluminant flicker to measure chromatic TCSFs is that the flicker is assumed to be invisible to the luminance pathway, so flicker detection must involve some chromatic mechanism or pathway (for review, see Stockman & Brainard, 2010). Equiluminance was determined separately for each observer using the minimum-motion technique of Anstis with interleaved, vertically orientated, 1-cycle per degree gratings that were cycled in quadrature spatial phase in opposite directions at 4 Hz over the same 5.7° diameter stimulus area. When the red and green grating components had a putative luminance imbalance, the interleaved gratings appeared to drift left or right depending upon which of the two components was greater in luminance, but when the interleaved gratings appeared motionless, they were assumed to be equal in luminance (for details of the method see, Anstis & Cavanagh, 1983; Cavanagh, MacLeod, & Anstis, 1987). The L:M equiluminant ratios calculated from the equiluminant settings were 1.70 for KR and 1.77 for JA.

Results

The results for JA in discriminating the rapid-on from the rapid-off stimuli on the basis of their mean hue differences are shown in Figure 1. Each panel shows the proportion of correct responses as a function of the cone modulation (logarithmic axis) with flicker frequency as the parameter indicated in each panel. Since no feedback was given to the observers, and the waveforms had identical physical mean chromaticity, we simply chose one sawtooth as the correct one. The top two rows in each figure are for L-cone stimulation, the bottom two rows, for M-cone stimulation. A logistic function with an unconstrained lapse rate (Wichmann & Hill, 2001a, 2001b) was fitted to each data set (black lines in each panel) merely to help summarize the data and the cone modulation that corresponded to the 75% correct level was estimated from the fitted curves in the panels. Each data point was based on three runs of 15 observations each.

Below 4 Hz, the mean hue change cannot be detected reliably at any modulation depth. At 4 Hz, performance is better than just guessing but never reaches 100% correct. Between 6.67 and 10 Hz, performance reaches 100% correct. However, from 11.43 Hz upward, performance fails to reach 100% correct and at 20 Hz, shifts in the mean hue are not reliably discriminated. Where the performance reaches 100%, the best-fitting functions are approximately parallel on these semilogarithmic coordinates so the effect of flicker frequency can be appropriately summarized by the differences across one performance level—we used the conventional 75% correct level. The raw data for the other observer, KR, are comparable and the results for both observers are summarized and indicated by triangles in separate panels of Figure 2.

The left and right panels of Figure 2 summarize the results for KR and JA, respectively. In both panels, $\log_{10}$ cone modulation sensitivity at 75% correct identification of the mean hue shift is shown as a function of frequency (Hz, logarithmic axis) using colored triangles. In these plots, sensitivity—defined as the reciprocal of the modulation corresponding to 75% correct discrimination—improves upwards. In both panels, the red triangles show the results for L-cone stimuli and the green triangles show the results for M-cone stimuli over the range of frequencies above 4 Hz for which the psychometric functions crossed 75% correct. There is little difference between L- and M-cone sensitivity within an observer, although L-cone sensitivity for both observers extends to higher frequencies. (The solid black line fitted to the data will be described subsequently.)

Figure 2 also shows each observer's sensitivity to L- and M-cone isolating sinusoidal flicker—half-filled red and green circles for L- and M-cone isolating stimuli, respectively. The error bars are ±1 standard error of the mean (*SEM*). There is relatively little difference between the observers with M-cone flicker (green dashed lines) but JA is the more sensitive with L-cone flicker (red dashed lines), particularly at the lowest frequencies. Both observers are more sensitive to L- than to M-cone flicker and clearly more sensitive to sinusoidal flicker than to the hue shifts produced by the sawtooth waveforms.

Sensitivity to equiluminant stimuli is shown as small orange diamonds. These sensitivities reflect sensitivity to chromatic flicker with no achromatic or luminance contribution. The vertical position of these data is essentially arbitrary because we do not know the effective chromatic contrast, but we have aligned them so that, if shifted horizontally, they coincide with the hue-shift discrimination data (see below).

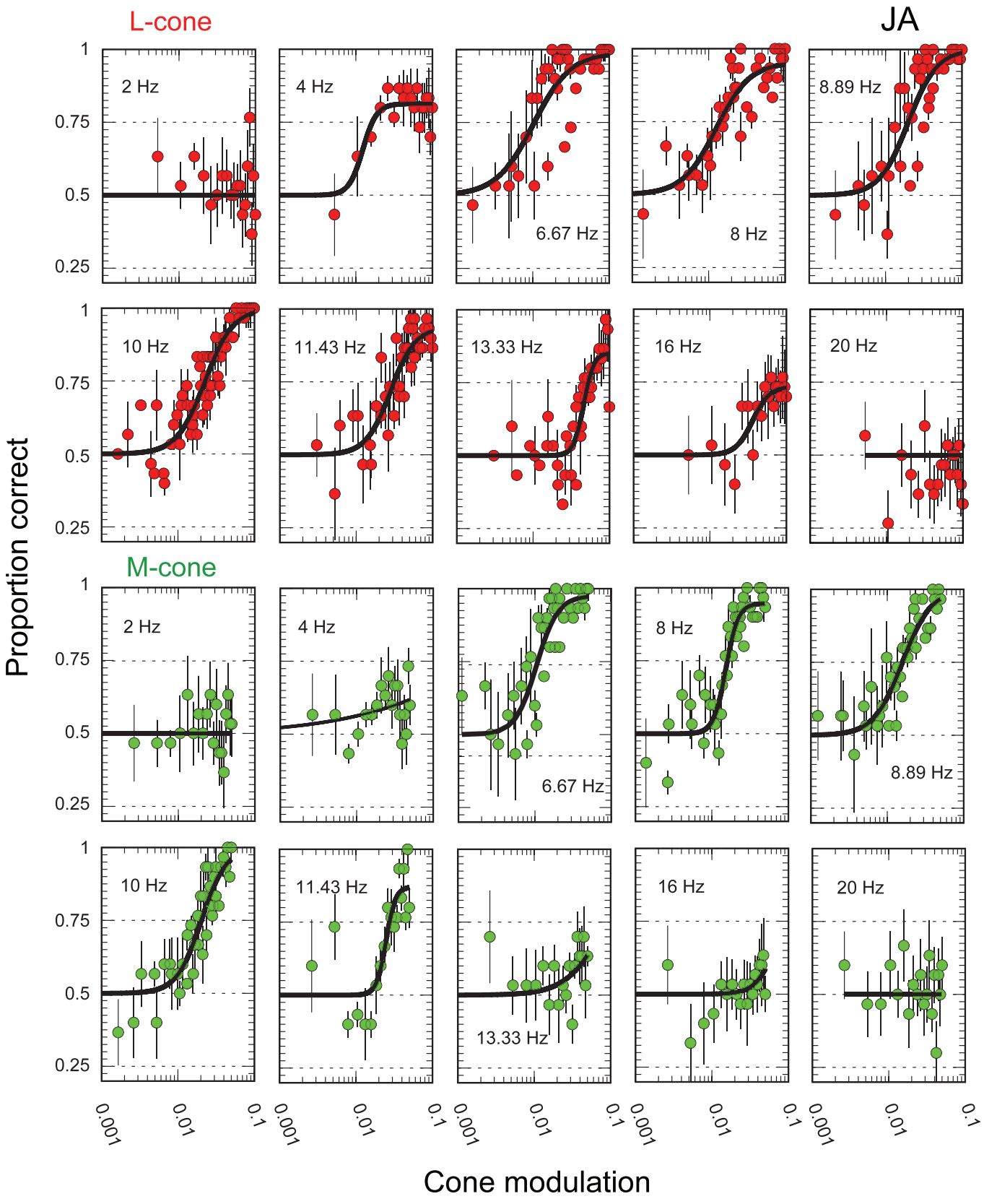

Figure 1. Results are shown for observer JA discriminating between matched rapid-on and rapid-off sawtooth waveforms as a function of their modulation, for L-cone stimuli in the top two rows and M-cone stimuli in the bottom two rows. Each panel shows the proportion of correct responses (linear scale) as a function of cone modulation (logarithmic scale) and each data point is based on 15 observations made on each of three runs. Results for different flicker frequencies ranging from 2 to 20 Hz are shown as indicated in each panel. The solid curves in each figure are the best-fitting logistic functions (with free lapse rates) for each set. The error bars represent ±1 *SEM* of the three runs.

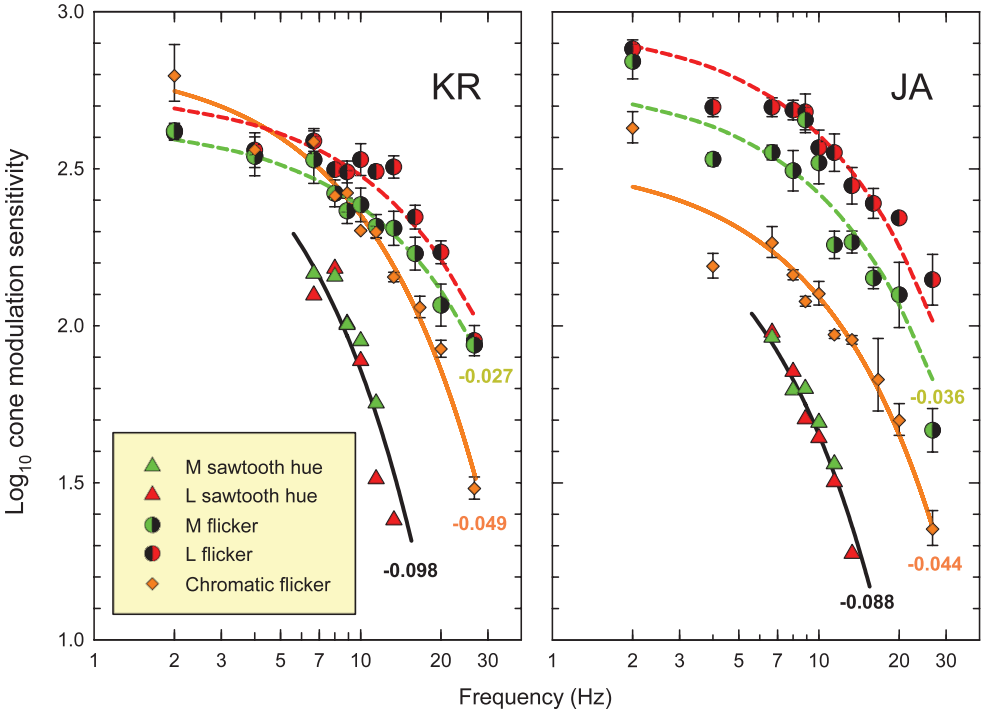

Figure 2. The two panels of Figure 2 summarize the discrimination results for each observer: KR in the left-hand panel and JA in the right-hand panel. In both panels, results for L-cone modulation are shown as red triangles, and M-cone modulation as green triangles. Log_{10} sensitivity (the logarithm of the reciprocal of the modulation corresponding to 75% correct) is plotted as a function of frequency (logarithmic scale). The figure also shows each observer's sensitivity to L-cone isolating sinusoidal flicker (half-colored red circles) and M-cone isolating sinusoidal flicker (half-colored green circles); the dashed red and dashed green lines are the best-fitting exponentials to the corresponding data. The orange diamonds show sensitivity to equiluminant red/green flicker and the solid orange line is the best fitting exponential to the orange diamonds. The black line aligned with the hue-shift data (triangles) is the exponential shown by the orange line with twice the exponent (see text). The error bars represent ±1 *SEM*.

As expected from preliminary observations, control experiments to measure the effects of different onset transients using two-alternative forced-choice procedures showed no significant differences between the hue discrimination thresholds between slowly-off and slowly-on sawtooth stimuli measured with the stimulus onset (a) at the beginning of the slowly rising or falling phase of the sawtooth, (b) at the middle of the slowly rising or falling phase of the sawtooth, or (c) gradually increased and decreased inside a raised-cosine envelope. This was true both for VL, who used the methods of limits, and for AS, who used a staircase procedure. The results for AS, for example, found no significant differences between the thresholds obtained with the different onset and offset envelopes using either L- or M-cone modulation at any frequency between 6.67 and 13.33 Hz.

Discussion

Cone-isolating and chromatic TCSFs

In Figure 2, the dashed red and green lines fitted to the cone modulation sensitivities, and the solid orange lines fitted to the chromatic sensitivities, are exponential functions of the form $s = a10^{bf}$, where s is the modulation sensitivity, f is frequency in Hz, and a and b are constants. Plotted as log modulation sensitivities against linear frequency, the function is a straight line:

$$\log_{10} s = bf + \log_{10} a. \quad (7)$$

The appropriateness of exponentials in describing the high-frequency slopes of TCSFs, in general, is the subject of a current project in our laboratory (Rider, Henning, & Stockman, 2016). All the data shown in this figure are well fit by exponentials, but could also be fit by more a conventional filter made up of a cascade of leaky integrators (see Watson, 1986). The choice of filter type does not affect our conclusions.

Equation 7 was used to fit the TCSF data. We found the best-fitting b value that jointly described *both* the M- and L-cone TCSFs for individual observers, with the result that the differences between the best-fitting values of $\log_{10} a$ provide an estimate of the observers' differences in sensitivity to L- and M-cone modulation.

For KR, the best-fitting value of b was −0.027 and her sensitivity for L-cone flicker was 0.099 $\log_{10}$ units greater than that for M-cone flicker. For JA, the best-fitting value of b was −0.036 and his sensitivity for L-

cone flicker was 0.187 $\log_{10}$ greater than that for M-cone flicker. The values of b, the slopes in Equation 7, are printed at the bottom of the curves in Figure 2.

Since both types of the cone-isolating stimuli we used, drive both chromatic and luminance mechanisms (e.g., Estevez & Cavonius, 1975), the L- and M-cone-isolating data reflect whichever mechanism is more sensitive—almost certainly the luminance mechanism at high frequencies and the chromatic mechanism at low frequencies—or a combination of the two when their sensitivities are similar. That the observers are more sensitive to L-cone flicker than to M-cone flicker may reflect the relative number of L and M cones in the observers' retinae (e.g., Rushton & Baker, 1964; Nerger & Cicerone, 1992; Brainard et al., 2000; Kremers, Scholl, Knau, Berendschot, & Sharpe, 2000; Hofer, Carroll, Neitz, Neitz, & Williams, 2005; Sharpe, Stockman, Jagla, & Jägle, 2005).

The solid orange lines are the best fits to the chromatic-flicker data, again using the simple exponential function of Equation 7. The best-fitting values of b that determine the rate of loss with increasing frequency are −0.044 and −0.049 for JA and KR, respectively. Thus, for chromatic flicker, sensitivity falls by a factor of two every 6.83 Hz for JA and every 6.08 Hz for KR. It can be seen in Figure 2, and these values confirm, that sensitivity to chromatic flicker falls faster than that for the cone-isolating stimuli, presumably because the data from the cone-isolating stimuli reflect, at the higher frequencies, the sensitivity of achromatic channels.

Hue-shift TCSFs

We cannot, of course, measure the effects of sawtooth cone-excitation waveforms directly—we can only infer their effects from the discrimination data. However, we can reasonably assume that the percentage of correct responses at a given flicker frequency depends on the size of the mean DC shift produced by the visual system at that frequency. How might we interpret the steep loss of sensitivity with frequency found for the hue-shift discrimination TCSFs—triangles in the panels of Figure 2? The black lines through the hue-shift data have double the negative slopes of the exponentials that describe the sinusoidal or first harmonic chromatic TCSFs; that is, from the orange to black lines, the slopes have been doubled from −0.049 to −0.098 for KR and from −0.044 to −0.088 for JA. The agreement between the black lines with the doubled slopes and the hue-shift TCSF data is suggestive. However, the agreement can be interpreted in two different ways, since the desired slope increase can be achieved either by halving the frequency or by doubling the $\log_{10}$ sensitivity.

Slope doubling is consistent with the hue-shift discrimination datorum depending on the attenuation of the second harmonic component of the sawtooth waveform after filtering by the chromatic filter. Plotted as a function of fundamental frequency, this is equivalent to dividing each frequency on the orange line by 2, and then shifting the $\log_{10}$ sensitivities to align with the hue-shift data as shown by the black lines. Such a dependence on the filtered second harmonic seems plausible, because, in the slowly-on and slowly-off waveforms, the third and first harmonics are in sine phase, but the second harmonics differ between the waveforms by 180° (see Table 1). Thus, if we consider only the lowest three components, the sawtooth waveforms will only be discriminable when their second harmonics reach a level that significantly alters the shapes of the waveforms and this level seems to be a multiple of that at which the component would be detected when presented by itself. Of course, a central nonlinearity must additionally transform the 180° phase difference of the second harmonics into the perceptually distinguishable shift in mean hue that we see.

On the other hand, the slope doubling is also consistent with the hue-shift discrimination data's depending on the square of the modulation of the first harmonic component of the sawtooth waveforms. This dependence is graphically equivalent to doubling each $\log_{10}$ cone modulation sensitivity on the orange line and then shifting the $\log_{10}$ sensitivities to align with the hue-shift data as shown by the black lines. A dependence on the square of the input modulation suggests that the hue-shift discriminability might depend on the first harmonic's approaching a saturation level produced by a smoothly compressive nonlinearity (Kelly, 1981). However, dependence of the measured hue shifts on the first harmonic rather than on the second seems less plausible, because the first harmonic alone does not allow discrimination between slowly-on and slowly-off waveforms.

Experiment II: Hue-shift discrimination and waveform slope

Introduction

In Experiment II we fixed the waveform modulation at 0.10 and varied the slope of the ramps of sawtooth waveforms to find the threshold for discriminating mean hue changes. In terms of the first and second harmonic components of these waveforms, the main effect of this manipulation is to hold the modulation of the first harmonic roughly constant while varying the

modulation of the second harmonic between 0% of the first harmonic (for a triangular wave) to as much as 50% for either sawtooth stimulus (see Figure 5, below).

Methods

We presented waveforms in the two 5.7° diameter semicircular hemifields separated by 0.6° of visual angle. Beginning with symmetrical triangular waveforms in both hemifields, the slopes of the waveforms were varied in equal-sized steps but opposite directions so that the stimulus in one hemifield was changed toward a slowly-off sawtooth and in the other toward a slowly-on sawtooth; the slowly-on direction was randomly assigned to one hemifield or the other. Both L-cone and M-cone modulation was used with the modulation fixed at 0.10. The number of frames in a stimulus cycle limited the slopes that were possible at a given frequency, but the limitations were identical for both waveforms. Varying the slopes of the waveforms in this way allowed the generation of psychometric functions relating the steeper slope of the waveform (in units of change in modulation per second) to the fraction of identifications of the redder hue in one of the asymmetric waveforms. Thus, in one randomly chosen hemifield a slowly-on waveform was presented, and in the other hemifield, slowly-off waveform was presented both with the same but opposite slopes. The observers were again asked to indicate the slowly-on waveforms for L-cone modulation or the slowly-off waveforms for M-cone modulation (i.e., the hemifield that appeared redder). In general, once the slope threshold had been exceeded for L-cone modulation, the hemifield containing the more slowly-on/rapidly-off flicker looked redder, whereas with M-cone stimuli, the more slowly-off/rapidly-on stimuli looked redder. No feedback was given; the observers were simply asked to indicate which half-field appeared redder. The modulations of the slowly-on and slowly-off pairs were varied together to generate psychometric functions relating the proportion of "redder" responses to the slope of the rapidly varying part of the waveform. Flicker frequencies ranging from 2 to 20 Hz were used, but interpretable discrimination data could be obtained only between 6.67 and 13.33 Hz.

The proportion of redder responses over 13 trials was plotted against the change of the rapid phase of the stimulus (in modulation per second) for each observer and for each frequency. The results for JA are shown in Figure 3. Best-fitting logistic functions were again used to determine the slope corresponding to 75% correct judgments and the results for three observers are summarized in Figure 4.

Results

Figure 3 shows the data for temporal frequencies ranging from 6.67 to 13.33 Hz for JA. Each panel shows the proportion of redder responses (linear scale) as a function of the change of the rapid phase of the stimulus (in modulation per second, logarithmic scale). The solid curves in each figure are again the best fitting logistic functions for each and the fit was used merely to determine the slope change corresponding to 75% correct judgments. Data for L-cone stimuli are shown in the left-hand column and for M-cone stimuli in the right-hand column. Each data point was based on 15 trials made on each of three separate runs and the error bars show ± 1 *SEM*. The data for KR and MS (not shown) are similar to those for JA.

Figure 4 shows the sawtooth *asymmetries* corresponding to the 75% correct discriminations plotted as a function of frequency (Hz) for KR in the top panel, JA in the middle panel, and MS in the bottom panel—red triangles for L-cone stimuli, and green triangles for M-cone stimuli. Both scales are linear. The asymmetry of the waveform corresponding to 75% correct judgments is indicated by the position of the peak or maximum of the waveform within the waveform's cycle. For example, in these units, a symmetrical triangular waveform reaches its maximum halfway through its period, so that its peak position is 0.5, whereas slowly-off stimuli reach their maxima earlier at values less than 0.5, and slowly-on waveforms reach their peak later at values greater than 0.5. The peak positions shown in Figure 4 are for the peaks of the slowly-off waveform member of the pair that were correctly discriminated 75% of the time (the position of the slowly-on waveform is always one minus this value).

The results for JA (middle panel) show a minimum asymmetry (i.e., the threshold position of peak closest to 0.5), where sensitivity to asymmetry is best, at about 10 Hz with greater asymmetry required below 10 Hz, and much greater asymmetries above 10 Hz. The results for L- and M-cone stimuli differ in the slope of the high-frequency arm. For KR (top panel) the minimum asymmetry appears to lie between 7 and 8 Hz with only the rapidly increasing high-frequency arm of the similar L- and M-cone datasets clearly visible. The frequency of best sensitivity for MS (bottom panel) is also approximately 8 Hz and the slopes of the high- and low-frequency arms of both the L- and M-cone data differ in slope. Unlike the data for JA, the slope of MS's high-frequency M-cone data is steeper than that for L-cones.

Discussion

The disparate forms of the datasets for individual observers shown in Figure 4 suggest that it will be

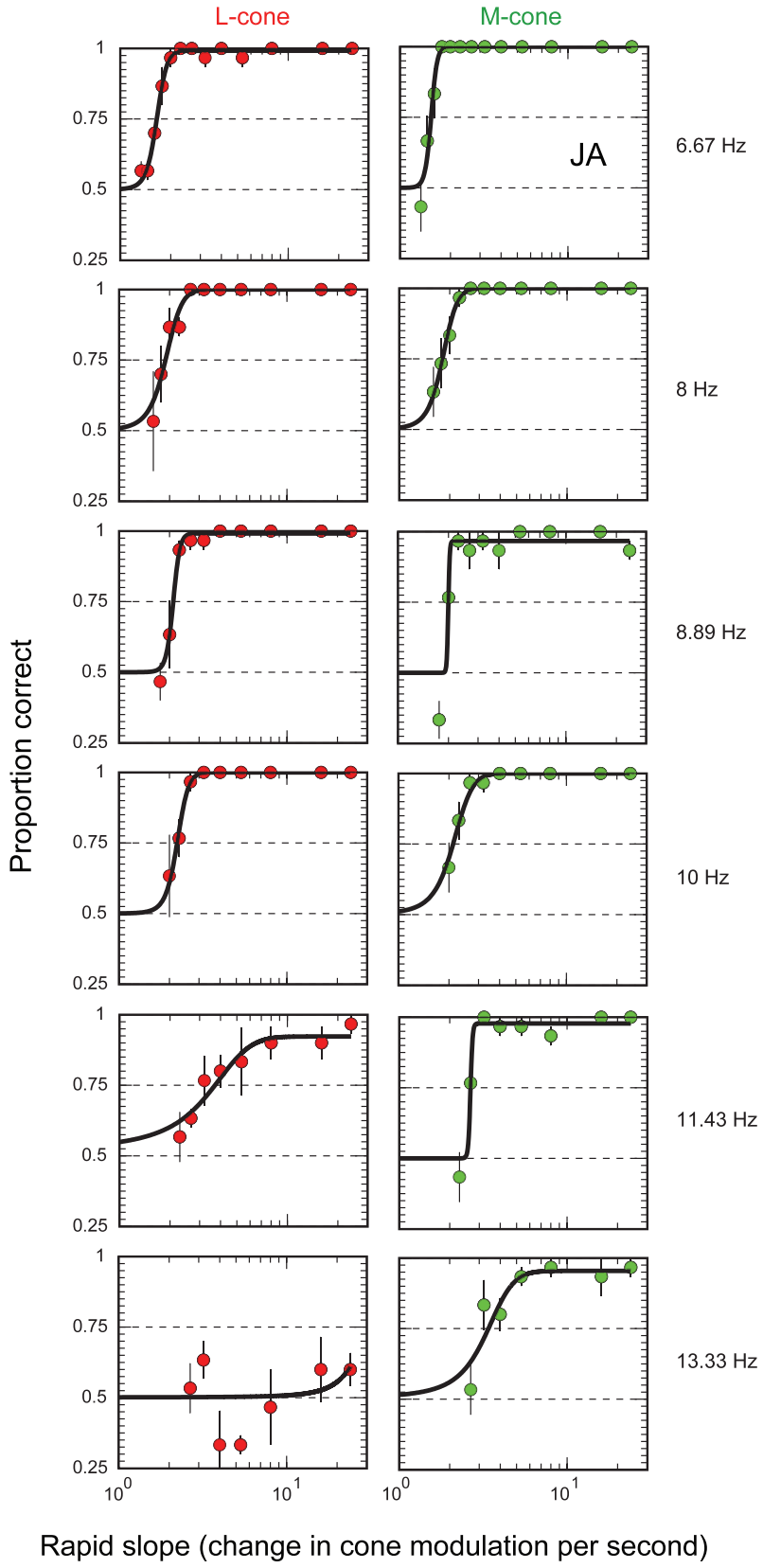

Figure 3. The panels of Figure 3 show the proportion of times JA correctly discriminates fast-on from fast-off waveforms as a function of the slope (change in modulation per second) of the more rapidly changing side of the paired sawtooth waveforms to be discriminated (logarithmic scale). Each data point is based on 15 observations made on each of three separate runs and the error bars represent ±1 *SEM* of the three runs. Performance for L-cone isolating stimuli is shown in the left-hand column and that for M-cone isolating stimuli in the right-hand column both for frequencies ranging from 6.67 to 13.33 Hz.

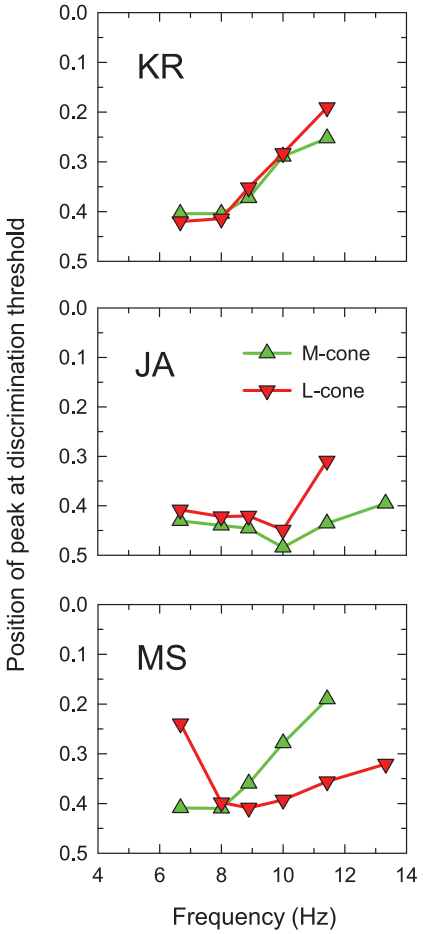

Figure 4. The panels of Figure 4 summarize the slope-discrimination data for KR (top panel), JA (middle panel, raw data in Figure 3), and MS (bottom panel). In each panel, the position of the peak at threshold of the more slowly-off waveform that corresponds to 75% correct discrimination is plotted as a function of frequency (Hz); the location of the peak is a measure of the asymmetry of the waveform. (The position of the peak of the more slowly-on waveform is always one minus the peak of the slowly-off waveform.) Both scales are linear. Thus, asymmetry in the pair of stimuli to be discriminated is indicated by the position within the half-cycle from 0.0 to 0.5 of the peak stimulus value of the more slowly-off waveform: 0.5 corresponds to symmetrical triangular waveforms, whereas 0.0 corresponds to slowly-off sawtooth waveforms. The observers were discriminating between randomly located hemifields containing matched pairs of more slowly-off and more slowly-on waveforms.

difficult to develop a simple model to account for the individual differences. Recall, however, that the results of Experiment I indicated the importance of the first and second harmonics of the sawtooth waveforms. Thus, if we represent the experiment results in terms of the sizes of those harmonics, it might reveal some data structure that is consistent across the three observers.

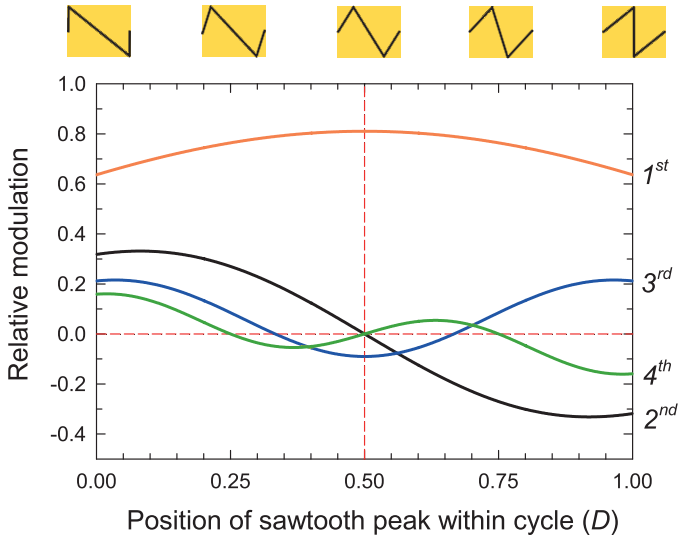

Figure 5. Modulation of the first (orange line), second (black line), third (blue line), and fourth (green line) harmonics of unit amplitude sawtooth-like stimuli as a function of the position, *D*, of the peak of the waveform within the cycle. The peak position varies from 0.0 (slowly-off sawtooth) through 0.5 (triangular) to 1.0 (slowly-on sawtooth) as illustrated by the icons at the top of the figure. A negative modulation corresponds to an 180° phase shift. Icons at the top illustrate waveforms corresponding to five selected asymmetries.

If D is the position of the peak of the sawtooth-like waveform of unit modulation, then the modulation (m) of the nth harmonic is given by:

$$m = \frac{2}{n^2\pi^2 D(1-D)}\sin(n\pi D). \quad (8)$$

The relation between D and m is shown for the first (orange line), second (black line), third (blue line), and fourth (green line) harmonics in Figure 5 where the modulation of the first four harmonics of sawtooth-like waveforms are shown as a function of the location of their peak. The icons at the top illustrate some of the waveforms. Note that second harmonic (and all even harmonics) shift in phase by 180° as D crosses 0.5. The 180° phase shift corresponds to the sign-change of the second harmonic in Figure 5.

The triangular wave, with a peak at 0.5, is symmetrical and is composed entirely of odd harmonics with zero amplitude second harmonic and all even harmonics (see also Equation 3). As the peak moves away from 0.5 in either direction, the waveforms become increasing asymmetrical as the second harmonic grows but in opposite phase above and below 0.5 (negative values for modulation indicate an 180° phase shift.) For the threshold discrimination measurements of Experiment II, the asymmetries range from about 0.2 to 0.8 and, over this range, Figure 5 indicates little

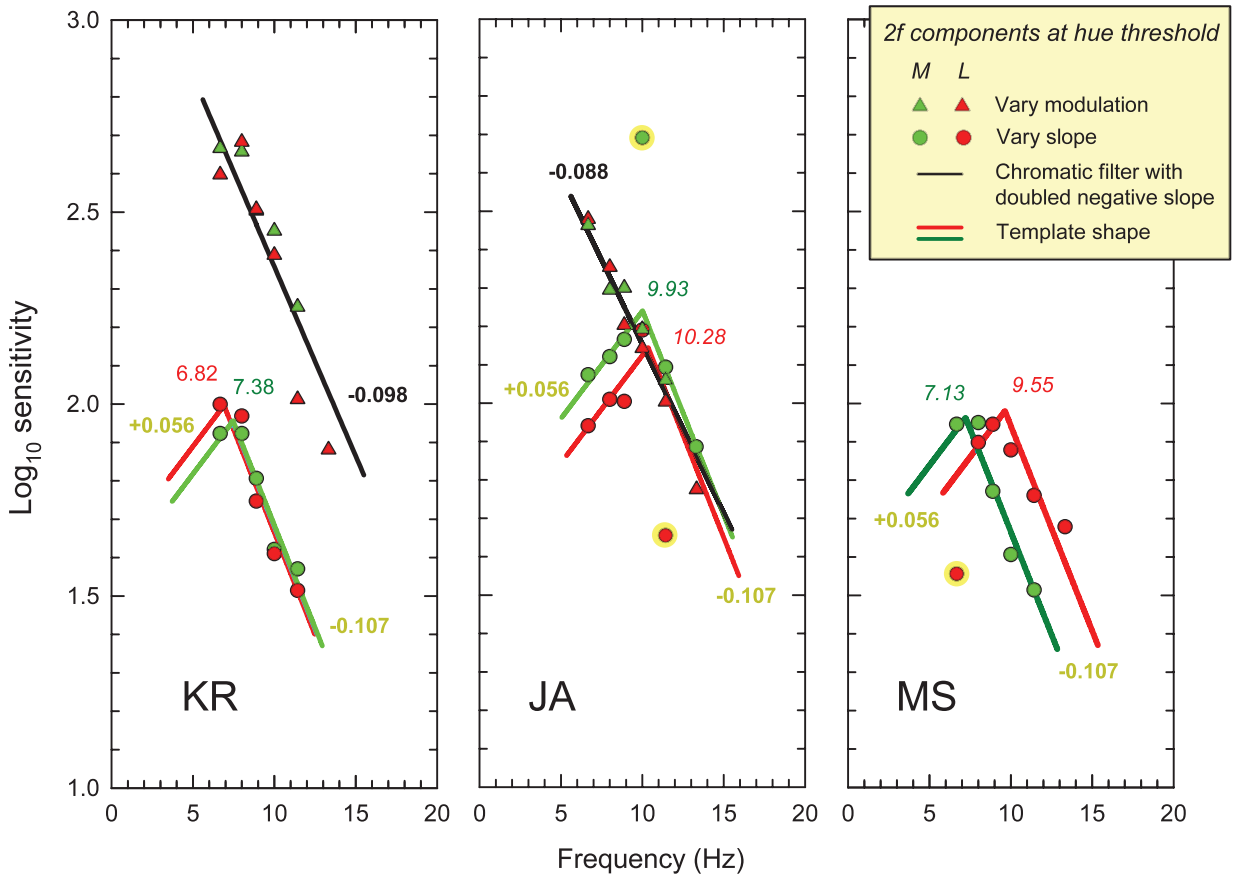

Figure 6. The logarithm of the reciprocal of the second harmonic modulation at the 75% correct "threshold" slope for discriminating the hue-shift from Experiment II (Figure 4) as a function of the fundamental frequency for L-cone isolating stimuli (red circles) and M-cone isolating stimuli (green circles) for KR (right panel), JA (middle panel), and MS (right panel). The solid red or green lines fitted to each set of data are empirically derived shape-invariant templates (see text for details); the frequencies at which the template peaks occur are noted in the figure (note that the three data points highlighted in yellow were not used to determine the template shapes or their fits). The hue-shift thresholds obtained by varying modulation from Experiment I (Figure 3) are shown as red (L-cone isolating stimuli) and green (M-cone isolating stimuli) triangles for KR and JA in the left and middle panels, respectively. The black lines fitted to those data show the effects of the chromatic filter at the second harmonic of each frequency. Neither thresholds nor filter are shown for MS, who did not carry out these measurements. The hue-shift thresholds and filters obtained by varying modulation have been shifted up by 0.5 $\log_{10}$ unit relative to their positions in Figure 2. This shift corrects for the difference between the sensitivity to the sawtooth waveform, which is plotted in Figure 2, and the reciprocal of the contrast of its second harmonic at the sawtooth's threshold contrast.

change in the amplitude of the first harmonic (solid red line), but over the same range the second harmonic is nearly linearly dependent on asymmetry. Thus, it is the second harmonic that is the significant frequency component with an amplitude that varies with peak position in the variable-slope experiment (note that the phase of the second harmonic is either 0° or 180° depending on whether the sawtooth is slowly-off or slowly-on). The fourth harmonic also varies with peak position around 0.5, but the relative modulation is small and falls to zero again at peak positions of 0.25 and 0.75.

Figure 6 shows the data from Figure 4 replotted as $\log_{10}$ sensitivity to the second harmonic as a function of frequency (logarithmic axis). Sensitivity to the second harmonic was calculated by taking the asymmetry that corresponds to 75% correct at each frequency, using Equation 8 to calculate the modulation of the second harmonic at that asymmetry, and measuring sensitivity as the reciprocal of that modulation. The M-cone and L-cone results are plotted as red and green circles, respectively (we discuss the template shapes shown by the solid red and green lines later).

Figure 6 also shows the hue-shift modulation thresholds for KR and JA from Figure 2 as red and green triangles for their L- and M-cone data, respectively; the black lines indicating the chromatic filters discussed as underlying these data are also from Figure

2 (orange lines). MS did not participate in Experiment I. Note that the triangles and black lines shapes have been shifted upward in Figure 6 by 0.5 $\log_{10}$ unit (a factor of $1/\pi$; see Equations 1 and 2) compared to Figure 2 to represent the true second harmonic sensitivity because the modulation of the second harmonic of a sawtooth waveform is about 0.5 $\log_{10}$ unit less than that of the overall waveform.

One interesting feature of Figure 6 is that, to a first approximation, the discrimination results of Experiment II appear shape-invariant in the sense that an appropriately horizontally and vertically shifted "template" can fit all the data. We used an iterative procedure to estimate the template shape (shown as the red and green lines aligned with each observers' data). Initially, all six sets of data were shifted vertically and horizontally by eye so that they subjectively aligned with each other. We excluded the three points outlined in yellow in Figure 6 from the alignments and curve-fitting procedures, as they distorted the fits. We then derived a template by curve fitting a peaked triangular function with best-fitting linear rising and falling slopes and intercepts to account for the subjectively aligned data (in the log-linear space). Next, we realigned the data with this new triangular function, also using a least-squares fitting procedure, and then derived another peaked triangular function to best fit the realigned data. The final triangular function fitted to the individual sets of M- and L-cone data is shown in Figure 6 as the solid red and green lines, respectively. Excluding the three highlighted points, the fits gave an R^2 value of 0.921. The template has a rising slope of +0.056 and falling slope of −0.107.

Although there are inflections in the data for KR and possibly for MS that suggest there is a loss in sensitivity at frequencies below the peak, such a loss is only clearly apparent in the data for JA. Importantly, though, the falling slope of −0.107 is consistent with the data for all three observers. Moreover, the slope of −0.107 is comparable to the falling slopes for the hue-shift discrimination data shown in Figure 2 (−0.098 and −0.088 for KR and JA, respectively). This similarity is consistent with the hue-shift discrimination's as a function both of waveform modulation and of waveform slope depending principally on the modulation of the second harmonic after the chromatic filter (orange lines, Figure 2). The alternative interpretation—that these high-frequency slopes depend on the square of modulation of the first harmonic—is much harder to justify since, for this experiment, it would require that the variation of the second harmonic modulation produced by varying the asymmetry of the waveform somehow also changes the first harmonic modulation.

The low-frequency branch of the template has a slope for JA of +0.056 that is approximately half that of the high-frequency arm common to all observers. Thus, below the peak JA needs increasingly more of the second harmonic to make the discrimination. We consider explanations for this sensitivity loss in the next section. However, it is perhaps worth noting that the amplitude of the effective first harmonic after the chromatic filter grows with decreasing frequency over this same region with approximately the same slope (see orange lines, Figure 2).

So far, our interpretation of the results has been mainly qualitative. What is clear from these results is that the hue-shift phenomenon is strongly dependent on the second harmonics of the slowly-off and slowly-on waveforms. In the next section, we attempt to provide models that are more concrete. The results seem to require a mechanism that follows the chromatic filter and is therefore relatively central in the chromatic processing stream.

General discussion

Here, we introduce two broad classes of model that might account for the subjective observations and the experimental data. For the cone-isolating stimuli used in our experiments, any successful model must relatively increase the mean cone excitation for slowly-on flicker, but decrease it for slowly-off flicker. Consequently, simple models built from linear filters will not work, because they do not alter the mean (time-average) cone excitation produced by continuously presented slowly-on and slowly-off flicker (given that, as we showed above, onset transients do not play a rôle). The change in the mean must be introduced by some form of nonlinearity somewhere in the chromatic processing stream that pushes the mean response in the direction of the slowly changing sawtooth ramp.

The first class of model incorporates a slew-rate limiting stage. This mechanism simply limits the rate at which the chromatic signal can change. The second class incorporates a stage with a nonlinearity that saturates or clips input signals symmetrically above and below the mean. Such a compressive nonlinearity, however, will not change the mean of slowly-off or of slowly-on waveforms, since the waveforms are mirror symmetric around their common mean. Nonetheless, a change in mean *will* occur if the second harmonic component of the sawtooth waveform is delayed, or advanced, prior to the saturating nonlinearity. Such delays, or equivalently, phase shifts, are a distinct possibility given the filtering that occurs in the chromatic pathway before the late nonlinearity (Petrova, Henning, & Stockman, 2013). We develop this idea below.

There is an overlap between the slew rate model and the compressive nonlinearity model, since the response of a slew-rate limited mechanism to a sawtooth stimulus is comparable to the response of a differentiator followed by a saturating nonlinearity (see also Cavanagh & Anstis, 1986). Steep slopes drive the differentiated response into a saturating region. Thus, a rapid change toward, for example, red, saturates the system in the "red" direction, so shifting the mean output in the opposite hue direction toward green. Such a model does indeed predict, at least qualitatively, the hue shifts we see for sawtooth waveforms. We consider first the slew-rate limiting model.

A slew-rate limiting model

The first model that we proposed to explain the shifts in mean hue produced by L- or M-cone modulated sawtooth stimuli incorporated a nonlinear mechanism in the chromatic pathway that places an upper limit on the rate at which the output can follow the input (e.g., Stockman & Ripamonti, 2014). The idea of such a slew-rate limit is common in electronics, particularly in the specification of linear amplifiers, but has been less frequently applied in visual science where its specific mention is sparse. Comparable phenomena in which sawtooth stimuli alter brightness rather than hue have been reported before, but have been explained in terms of successive contrast (Walker, 1974) or sustained and saturating transient responses (Cavanagh & Anstis, 1986). Cavanagh and Anstis (1986) argue that their model was "analogous to slew-rate limiting in an amplifier" (p. 905).

Figure 7 illustrates the effect of a simple slew-rate limit on the sum of the first and second harmonic components of three different 8-Hz L- and M-cone modulations. The three waveforms are: a slowly-off/rapidly-on sawtooth waveform (upper row), a symmetrical "triangle" waveform (middle row), and a slowly-on/rapidly-off waveform (bottom row), all plotted as a function of time (seconds). Given the importance of the first and second harmonics in producing the hue shifts, we have removed the third and higher harmonics of the three types of waveforms in the simulations (see Equations 1 to 3). Thus, the triangle wave becomes a sinusoid and the slowly-off and slowly-off waveforms become first and second harmonics in the amplitude ratio of 2:1. The stimuli (black lines) are plotted as cone excitations relative to a mean excitation of unity (horizontal dashed lines). The limiting slope used in these simulations is plotted in red in the inset at the top of the figure and, in this case, is 3.0 units s^{-1} for both positive- and negative-going changes (where the units are the change in cone excitations). If we impose the slew-rate limitations shown in the inset on the three input waveforms, the output waveforms shown by the solid white lines are produced. Changes in L-cone driven response (left-hand column) or M-cone-driven response (right-hand column) are plotted. We call these cone-driven responses but in the simulations they are the output of the slew-rate limited mechanism we use to model the cone response, which, of course, is likely to be postreceptoral. The background colors in Figure 7 represent the hue directions (redward or greenward) related to changes in L-cone or M-cone excitation relative to the yellow appearing mean excitation (horizontal black dashes). An increase in cone excitation above the mean is plotted as positive, and a decrease below the mean as negative. Note that in each case, the waveforms start at the mean level. Had we started them at a different level, the output waveforms would have taken more cycles to reach the same asymptotic waveform.

The dashed white lines show the mean response after the slew-rate limiting mechanism and, in this model, we associate the shifts in mean hue reported by our observers with the shift produced by the slew-rate limit. For the asymmetrical (sawtooth) waveforms in the top and bottom panels there is a shift in the mean and time-varying components of the output towards the more slowly changing side of the sawtooth. The shifts occur because the slew-rate limit follows the slowly changing side of the sawtooth more closely that the rapidly changing side. The directions of the shifts are consistent with the hue shifts reported by our observers. With the symmetrical waveform of the middle panel, there is no shift in either the mean or the time-varying components of the slew-rate limited output. This result is again in agreement with the lack of a mean hue shift reported by our observers.

Other predictions of comparable simulations obtained using the slew-rate model are worth summarizing. In general, a slew-rate limit causes a shift in the mean hue when the steeper slope of asymmetric input waveforms (such as the slowly-off and slowly-on waveforms shown in Figure 7) exceeds the slew rate limit. Further increases in either the waveform modulation or the waveform frequency will then increase the waveform slopes, and cause the mean hue-shift to increase until the shallower slope of the waveform *also* exceeds the slew-rate limit. Once both slopes exceed the slew-rate limit, the output waveform becomes triangular. If the modulation is still further increased (at constant frequency), the amplitude of the triangular waveform and the hue shift remain relatively constant. If instead the frequency is still further increased, the amplitude of the triangular waveform and the hue shift both *fall* with frequency, since the waveform period restricts by how much the limited rate can rise or fall during each waveform cycle. Thus,

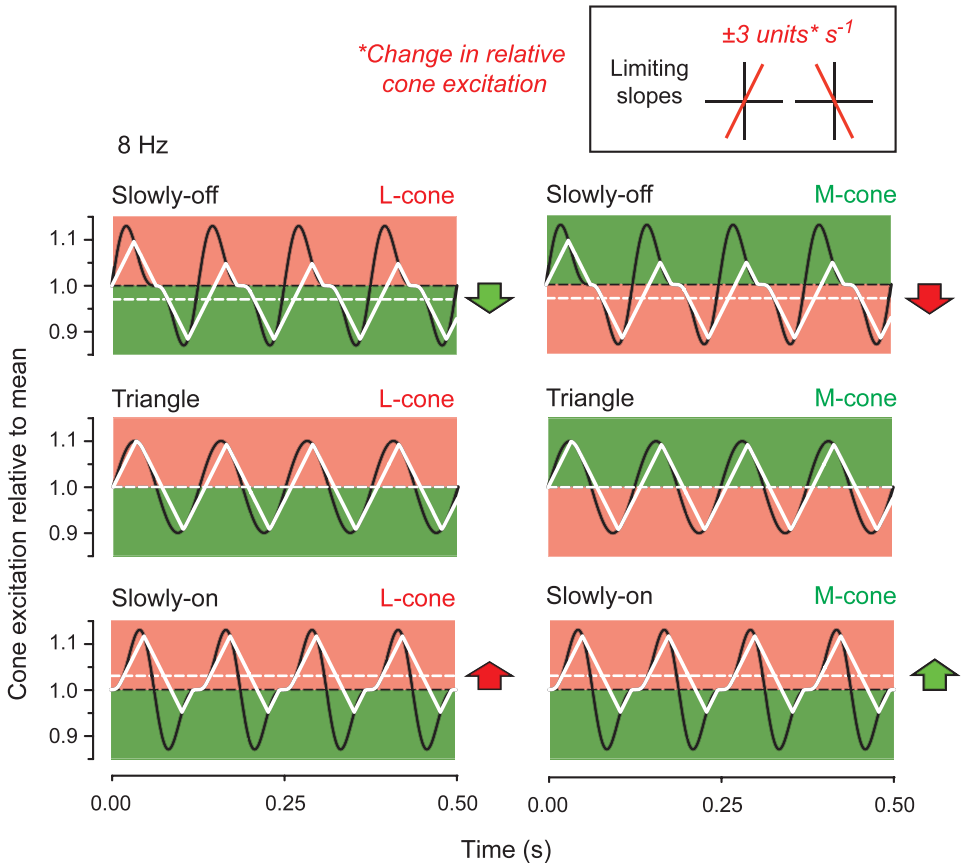

Figure 7. Each panel shows the sum of the first and second harmonics of a sawtooth stimulus (black solid lines) as the cone excitation relative to the mean cone excitation (dashed horizontal black lines) plotted as a function of time for four cycles of 8-Hz sawtooth waveforms (top and bottom panels) and of a triangular waveform of the same frequency, which, having a zero amplitude second harmonic, is a sinusoid (middle panels). The difference in effective relative cone excitation after the slew-rate limit from the mean is also illustrated as solid white lines with its mean deviation shown as dashed horizontal white lines. The colored backgrounds represent the directions of the hue shifts related to the mean stimulus for L-cone isolating stimuli (left-hand column) or M-cone isolating stimuli (right-hand column). Thus, in all cases, the mean stimulus hue (seen with no flicker) at 1.0 is yellow and positive deviations are in the "on" direction—toward red for L cones and toward green for M cones. For the illustration in the case of the sawtooth waveforms, it is assumed that the chromatic mechanisms cannot follow the rapid change but can just follow the slow change (i.e., the slow change is just at the slew-rate limit of ± 3.0 units s^{-1}, where the units are the change in relative cone excitation) as shown above the right-hand column. For the triangular (or sinusoidal) waveform, the rate limiting prevents the chromatic mechanisms accurately following most of either the rising or the falling parts of the stimulus.

we might suppose that the peaks of the peaked hue-discrimination functions shown in Figure 6 (red and green lines) correspond to the frequency and modulations at which the overall slope of the shallower slope of threshold stimuli match the slew-rate limit, provided that the slew-rate limited model is appropriate.

We now turn to an alternative model.

Instantaneous nonlinearity

Although the simplicity of the slew-rate limit model is compelling, it is difficult to assess the model without using simulations, and it is hard to link the model to known physiological processes. Models incorporating instantaneous static nonlinear processes are relatively simple and have frequently been used in modeling vision (e.g., Spekreijse & Reits, 1982), and have presumed physiological counterparts (e.g., Albrecht & Hamilton, 1982).

Figure 8 allows a comparison between simulations of a symmetrical hard-limiting saturation that limits excursions beyond 0.075 units from the mean (left-hand column) and a symmetrical mechanism limiting slew-rates at ± 2 units s^{-1} (right-hand column). All the panels show 0.5 s of the sum of an 8-Hz fundamental of fixed amplitude and a second harmonic of one quarter that amplitude. This amplitude was chosen to reflect the lower amplitude of the second harmonic in the

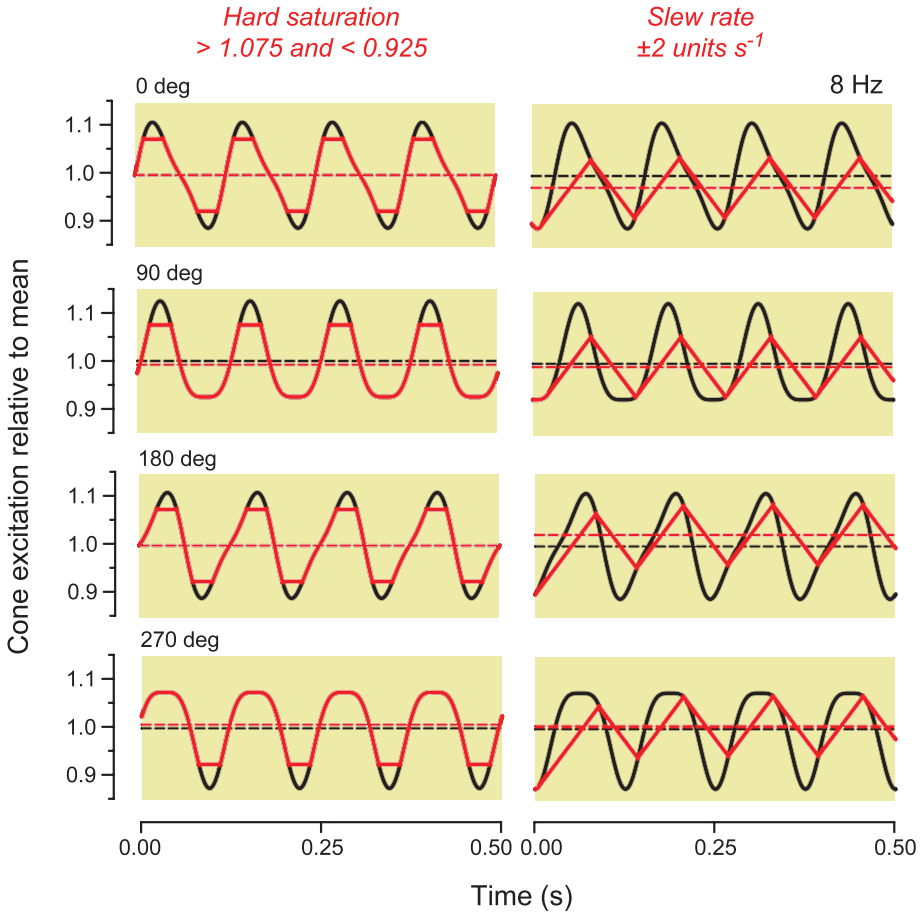

Figure 8. The left- and right-hand columns show simulations for a symmetrical hard saturating and a slew-rate limiting mechanism, respectively, in response to an 8-Hz first harmonic added to a second harmonic having one quarter the modulation of the first. Each row shows the results for a second harmonic added in a different phase—from 0° in the top row to 270° in the bottom. The black lines in each panel show the input stimuli and the red lines the outputs of the mechanisms. The horizontal dashed red lines indicate the DC shifts in the outputs.

stimulus and, as we suspect, its further attenuation relative to the fundamental by the chromatic filter. The input waveforms are shown in black and the output waveforms are shown in red; their mean levels are shown as the black and red dashed lines, respectively. Each row shows the effects on the sum of the first and second harmonics produced by a different phase delay of the second harmonic—from the top to the bottom panel with appropriate labels: 0° (slowly-off), 90° (peaks-align), 180° (slowly-on) and 270° (troughs-align).

Now, as outlined above, a saturating nonlinearity that is symmetrical around the mean will not change the mean output produced by a sawtooth waveform. This is illustrated in the first and third panels in the left-hand column of Figure 8, which show the first and second harmonics of slowly-off and slowly-on sawtooth waveforms, respectively. For the slowly-off and slowly-on waveforms, the output mean is the same as the input mean. If, however, the second harmonic of either the slowly-off or the slowly-on waveforms is delayed by 90°, as shown in the second and fourth panels, then the shapes of the waveforms become asymmetrical around the mean and clipping alters the mean output signal. Thus, the symmetrical hard-limiting saturation mechanism can produce DC shifts provided the relative phases of the components at its input are appropriate.

How do comparable phase shifts affect the slew-rate model predictions? The right-hand column of Figure 8 simulates the effect of a slew-rate limiting mechanism (of ± 2 s^{-1}). Again, the modulation of the second harmonic is one quarter of that of the first harmonic. In this case, the DC shifts are greater for the slowly-off and slowly-on waveforms than for the peaks-align and troughs-align waveforms. On the face of it, then, Figure 8 suggests that the slew-rate limit better approximates our results, since it predicts hue shifts with the slowly-off and slowly-on waveforms, whereas the static nonlinearity does not. However, since the chromatic filter that precedes the nonlinear stage (Petrova et al., 2013), must introduce phase shifts between the first and

second harmonics of the sawtooth waveforms, we cannot be certain which of these two models is the more likely. In a subsequent paper, we investigate the effect of varying the phase of the second harmonic on the mean and time-varying hue appearances of these waveforms (Stockman, Henning, West, Rider, & Ripamonti, 2017).

Figure 8 can help to illustrate how a slew-rate limited model for these waveforms has a qualitatively similar response to a differentiator followed by a saturating nonlinearity. Differentiating a sine wave produces a cosine wave that increases in amplitude in proportion to frequency; that is, $\frac{d}{dt}\sin(2\pi ft) = 2\pi f\cos(2\pi ft)$, where (as above) f is frequency in Hz and t is time in seconds. Thus, after differentiation both the first and second harmonics of the waveforms in Figure 8 are phase advanced by 90° and the size of the second harmonic is doubled relative to that of the first. In terms of the composite waveforms (and ignoring the amplitude doubling of the second harmonic), the differentiation changes the slowly-off waveform into the peaks-align waveform, the peaks-align into the slowly-on, the slowly-on into the troughs-align, and the troughs-align to the slowly-off. Thus, with respect to the input waveforms, the composite waveforms that are most clipped by a saturating nonlinearity following differentiation are the slowly-off and slowly-on waveforms, which are the same waveforms most affected by the slew-rate limit. A bandpass temporal frequency response, which is often associated with early temporal processing in the retina (e.g., Stockman, Petrova, & Henning, 2014), will act like a differentiator at low frequencies. However, to be consistent with our data, this has to be reconciled with the overall frequency response being low-pass (see Figure 2).

Many other models were also considered, such as ones that selectively affected the phases of the sawtooth waveforms above and below the mean by separate compression or by separate slew rates, but the additional complexities did not simplify or significantly improve the model predictions.

Conclusions

A nonlinear mechanism in the chromatic pathway shifts the mean hue of sawtooth flickering L- and M-cone lights. Two classes of explanatory model are consistent with the hue shifts. In one, a nonlinear stage limits the rate of change of hue, and in the other, a nonlinear stage symmetrically limits hue excursions from the mean. Since the two models make very different predictions about the dependence of the hue shifts on the phase of the second harmonic, one way of testing these models will be to investigate the effect of varying the second harmonic phase on the mean and time-varying hue appearance of these waveforms.

Keywords: color, chromatic flicker, nonlinearity, temporal vision

Acknowledgments

This work was supported by Grants BB/1003444/1 and BB/M00211X/1 from the BBSRC. We thank Jonathan Aboshiha and Magda Sbai for being observers in the experiments. We also grateful to Rhea Eskew and Donald MacLeod for helpful comments on the manuscript.

Commercial relationships: none.
Corresponding author: Andrew Stockman.
Email: a.stockman@ucl.ac.uk.
Address: UCL Institute of Ophthalmology, University College London, London, UK.

References

Albrecht, D. G., & Hamilton, D. B. (1982). Striate cortex of monkey and cat: Contrast response function. *Journal of Neurophysiology*, *48*(1), 217–237.

Anstis, S. M., & Cavanagh, P. (1983). A minimum motion technique for judging equiluminance. In J. D. Mollon & L. T. Sharpe (Eds.), *Colour vision: Physiology and psychophysics*. New York: Academic Press.

Billock, V. A., Gleason, G. A., & Tsou, B. H. (2001). Perception of forbidden colors in retinally stabilized equiluminance images: An indication of softwired cortical color opponency. *Journal of the Optical Society of America A*, *10*, 2398–2403.

Brainard, D. H., Roorda, A., Yamauchi, Y., Calderone, J. B., Metha, A., Neitz, M., ... Jacobs, G. H. (2000). Functional consequences of the relative numbers of L and M cones. *Journal of the Optical Society of America A*, *17*(3), 607–614.

Brindley, G. S., Du Croz, J. J., & Rushton, W. A. H. (1966). The flicker fusion frequency of the blue-sensitive mechanism of colour vision. *Journal of Physiology*, *183*(2), 497–500.

Cavanagh, P., & Anstis, S. M. (1986). Brightness shift in drifting ramp gratings isolates a transient mechanism. *Vision Research*, *26*(6), 899–908.

Cavanagh, P., MacLeod, D. I. A., & Anstis, S. M. (1987). Equiluminance: Spatial and temporal fac-

tors and the contribution of blue-sensitive cones. *Journal of the Optical Society of America A*, *4*(8), 1428–1438.

Crane, H. D., & Piantanida, T. (1983). On seeing reddish green and yellowish blue. *Science*, *221*(4615), 1078–1080.

de Lange, H. (1958). Research into the dynamic nature of the human fovea-cortex systems with intermittent and modulated light. II. Phase shift in brightness and delay in color perception. *Journal of the Optical Society of America*, *48*, 784–789.

Estevez, O., & Cavonius, C. R. (1975). Flicker sensitivity of the human red and green color mechanisms. *Vision Research*, *15*(7), 879–881.

Estévez, O., & Spekreijse, H. (1982). The "silent substitution" method in visual research. *Vision Research*, *22*, 681–691.

Green, D. G. (1969). Contrast sensitivity of the human peripheral retina. *Vision Research*, *9*(8), 947–952.

Hofer, H. J., Carroll, J., Neitz, J., Neitz, M., & Williams, D. R. (2005). Organization of the human trichromatic cone mosaic. *Journal of Neuroscience*, *25*(42), 9669–9679.

Kelly, D. H. (1981). Nonlinear visual responses to flickering sinusoidal grating. *Journal of the Optical Society of America*, *71*, 1051–1055.

Kelly, D. H., & van Norren, D. (1977). Two-band model of heterochromatic flicker. *Journal of the Optical Society of America*, *67*(8), 1081–1091.

King-Smith, P. E. (1975). Visual detection analysed in terms of luminance and chromatic signals. *Nature*, *255*(5503), 69–70.

King-Smith, P. E., & Carden, D. (1976). Luminance and opponent-color contributions to visual detection and adaptation and to temporal and spatial integration. *Journal of the Optical Society of America*, *66*(7), 709–717.

Kremers, J., Scholl, H. P. N., Knau, H., Berendschot, T. T. J. M., & Sharpe, L. T. (2000). L/M cone ratios in human trichromats assessed by psychophysics, electroretinography and retinal densitometry. *Journal of the Optical Society of America A*, *17*(3), 517–526.

Lee, B. B., Sun, H., & Zucchini, W. (2007). The temporal properties of the response of macaque ganglion cells and central mechanisms of flicker detection. *Journal of Vision*, *7*(14):1, 1–16, doi:10.1167/7.14.1. [PubMed] [Article]

Levitt, H. (1971). Transformed up–down methods in psychoacoustics. *Journal of the Acoustical Society of America*, *49*(2), Suppl 2, 466–477.

Metha, A. B., & Mullen, K. T. (1996). Temporal mechanisms underlying flicker detection and identification for red-green and achromatic stimuli. *Journal of the Optical Society of America A*, *13*(10), 1969–1980.

Nerger, J. L., & Cicerone, C. M. (1992). The ratio of L cones to M cones in the human parafoveal retina. *Vision Research*, *32*(5), 879–888.

Noorlander, C., Heuts, M. J. G., & Koenderink, J. J. (1981). Sensitivity to spatiotemporal combined luminance and chromaticity contrast. *Journal of the Optical Society of America*, *71*(4), 453–459.

Petrova, D., Henning, G. B., & Stockman, A. (2013). The temporal characteristics of the early and late stages of the L- and M-cone pathways that signal color. *Journal of Vision*, *13*(4):2, 1–26, doi:10.1167/13.4.2. [PubMed] [Article]

Regan, D., & Tyler, C. W. (1971). Some dynamic features of colour vision. *Vision Research*, *11*(11), 1307–1324.

Rider, A. T., Henning, G. B., & Stockman, A. (2016). Light adaptation and the human temporal response revisited. *Journal of Vision*, *16*(12):387, doi:10.1167/16.12.387. [Abstract]

Rushton, W. A. H., & Baker, H. D. (1964). Red/green sensitivity in normal vision. *Vision Research*, *4*(1–2), 75–85.

Sharpe, L. T., Fach, C. C., Nordby, K., & Stockman, A. (1989). The incremental threshold of the rod visual system and Weber's law. *Science*, *244*(4902), 354–356.

Sharpe, L. T., Stockman, A., Jagla, W., & Jägle, H. (2005). A luminous efficiency function, *V*(l)*, for daylight adaptation. *Journal of Vision*, *5*(11):3, 948–968, doi:10.1167/5.11.3. [PubMed] [Article]

Smith, V. C., Bowen, R. W., & Pokorny, J. (1984). Threshold temporal integration of chromatic stimuli. *Vision Research*, *24*(7), 653–660.

Spekreijse, H., & Reits, D. (1982). Sequential analysis of the visual evoked potential system in man: Nonlinear analysis of a sandwich system. *Annals of the New York Academy of Sciences*, *388*, 72–97.

Sternheim, C. E., Stromeyer, C. F., III, & Khoo, M. C. K. (1979). Visibility of chromatic flicker upon spectrally mixed adapting fields. *Vision Research*, *19*(2), 175–183.

Stockman, A., & Brainard, D. H. (2010). Color vision mechanisms. In M. Bass, C. DeCusatis, J. Enoch, V. Lakshminarayanan, G. Li, C. Macdonald, V. Mahajan & E. van Stryland (Eds.), *The Optical Society of America handbook of optics, 3rd edition, Volume III: Vision and vision pptics* (pp. 11.11–11.104). New York: McGraw Hill.

Stockman, A., Henning, G. B., West, P., Rider, A. T., & Ripamonti, C. (2017). Hue shifts produced by temporal asymmetries in chromatic signals depend on the alignment of the first and second harmonics. *Journal of Vision*, *17*(9):3, 1–23, doi:10.1167/17.9.3.

Stockman, A., MacLeod, D. I. A., & DePriest, D. D. (1991). The temporal properties of the human short-wave photoreceptors and their associated pathways. *Vision Research*, *31*(2), 189–208.

Stockman, A., Petrova, D., & Henning, G. B. (2014). Color and brightness encoded in a common L- and M-cone pathway with expansive and compressive nonlinearities? *Journal of Vision*, *14*(3):1, 1–32, doi: 10.1167/14.3.1. [PubMed] [Article]

Stockman, A., & Ripamonti, C. (2014). Red-green flicker is encoded by a peak detector and limited by slew rate. *Journal of Vision*, *14*(10):592, doi:10. 11657/14.10.592. [Abstract]

Stockman, A., & Sharpe, L. T. (2000). Spectral sensitivities of the middle- and long-wavelength sensitive cones derived from measurements in observers of known genotype. *Vision Research*, *40*(13), 1711–1737.

Stockman, A., Sharpe, L. T., Tufail, A., Kell, P. D., Ripamonti, C., & Jeffery, G. (2007). The effect of sildenafil citrate (Viagra®) on visual sensitivity. *Journal of Vision*, *7*(8):4, 1–15, doi:10.1167/7.8.4. [PubMed] [Article]

Stockman, A., Smithson, H. E., Michaelides, M., Moore, A. T., Webster, A. R., & Sharpe, L. T. (2007). Residual cone vision without a-transducin. *Journal of Vision*, *7*(4):8, 1–13, doi:10.1167/7.4.8. [PubMed] [Article]

Stockman, A., Smithson, H. E., Webster, A. R., Holder, G. E., Rana, N. A., Ripamonti, C., & Sharpe, L. T. (2008). The loss of the PDE6 deactivating enzyme, RGS9, results in precocious light adaptation at low light levels. *Journal of Vision*, *8*(1):10, 1–10, doi:10.1167/8.1.10. [PubMed] [Article]

Tolhurst, D. J. (1977). Colour-coding properties of sustained and transient channels in human vision. *Nature*, *266*(5599), 266–268.

Walker, J. T. (1974). A new rotating gradient disk: Brightness, flicker, and brightness aftereffects. *Vision Research*, *14*(3), 223–228.

Walraven, P. L., & Leebeek, H. J. (1964). Phase shift of sinusoidally alternating colored stimuli. *Journal of the Optical Society of America*, *54*, 78–82.

Watson, A. B. (1986). Temporal sensitivity. In K. Boff, L. Kaufman, & J. Thomas (Eds.), *Handbook of perception and human performance* (Vol. 1, pp. 6.1–6.43). New York: Wiley.

Watson, A. B., & Yellott, J. I. (2012). A unified formula for light-adapted pupil size. *Journal of Vision*, *12*(10):12, 1–16, doi:10.1167/12.10.12. [PubMed] [Article]

Wichmann, F. A., & Hill, N. J. (2001a). The psychometric function: I. Fitting, sampling, and goodness-of-fit. *Perception and Psychophysics*, *63*(8), 1293–1313.

Wichmann, F. A., & Hill, N. J. (2001b). The psychometric function: II. Bootstrap-based confidence intervals and sampling. *Perception and Psychophysics*, *63*(8), 1314–1329.

Yeh, T., Lee, B. B., & Kremers, J. (1995). Temporal response of ganglion cells of the macaque retina to cone-specific modulation. *Journal of the Optical Society America A*, *12*(3), 456–464.